

# Ellipsometric analysis of ion-implanted polycrystalline silicon films before and after annealing

Emmanouil Lioudakis<sup>a,\*</sup>, Androula Nassiopoulou<sup>b</sup>, Andreas Othonos<sup>a</sup>

<sup>a</sup> Department of Physics, University of Cyprus, P.O. Box 20537, 1678, Nicosia, Cyprus

<sup>b</sup> IMEL/NCSR Demokritos, P.O. Box 60228, 15310, Aghia Paraskevi, Athens, Greece

Received 7 September 2004; received in revised form 9 March 2005; accepted 22 August 2005

Available online 16 September 2005

## Abstract

A study of arsenic ion-implanted polycrystalline silicon films before and after annealing at various temperatures has been performed using spectroscopic ellipsometry in the ultraviolet to the visible spectral region. Using the Bruggeman effective medium approximation, an optical/structural model is presented for all the annealed samples explaining the measurements. Ellipsometric measurements reveal important structural changes as a function of annealing temperature which provide an interesting insight into the annealing kinetics of ion-implanted polycrystalline silicon films. This work also demonstrates the importance of spectroscopic ellipsometry in determining non-destructively the dielectric functions in materials that have undergone complex processing.

© 2005 Elsevier B.V. All rights reserved.

PACS: 123; 214; 17

Keywords: Ellipsometry; Ion implantation; Annealing; Polycrystalline silicon

## 1. Introduction

Polycrystalline silicon is a material of great importance in microelectronics, photovoltaics and display technologies. It is commonly used in thin film transistors and as a gate material in metal-oxide-semiconductor technology. Ion implantation of crystalline or polycrystalline silicon is currently used to alter and tailor the conductivity of the material. Ion implantation, however, depending on the dose and implantation energy, may partially or completely alter the crystal structure of the material, causing degradation of its electrical properties [1,2]. In many cases this is unacceptable, and annealing is often utilized to recrystallize the implanted damaged material.

Although the temperature of 800 °C is considered to be the threshold above which the damaged material is reconstructed and returned to its original crystal structure, structural changes may occur in such samples even at annealing temperatures below 800 °C. These changes may not be easily observable with optical techniques such as Raman scattering [3]. However, recently with the introduction of microcomputers and computer

interfaces, spectroscopic ellipsometry [4–7] has been established to be a very effective technique for the characterization of thin surface layers [8] with very high sensitivity and accuracy.

In this paper, we report on an ellipsometric analysis in the ultraviolet to the visible spectral region of polycrystalline silicon films highly implanted with arsenic ions and annealed at various temperatures in the range of 300 to 1100 °C. We demonstrate the sensitivity of the technique to the structural changes induced by annealing in the polycrystalline ion-implanted samples. Furthermore, we formulate an optical model to describe these structural changes, thereby demonstrating the possibility of using this technique as a powerful non-destructive characterization method in the processing of these samples.

## 2. Experimental details

In this work, measurements on ion-implanted polycrystalline silicon films grown by low pressure chemical vapor deposition were performed using a spectroscopic ellipsometer (type GES5-SOPRA). The system consists of a broadband light source followed by a polarizer and a retarder, which are attached to the incoming section of the ellipsometer. The

\* Corresponding author. Fax: +357 22892821.

E-mail address: [mlioud@ucy.ac.cy](mailto:mlioud@ucy.ac.cy) (E. Lioudakis).

polarized broadband light is then incident to the sample and the reflected beam, after passing through an analyzer, enters a monochromator in order to select the spectrum region of interest. Light intensity is measured by a detector, which is placed after the monochromator.

The samples used in this work were 1  $\mu\text{m}$  thick polycrystalline silicon films deposited on crystalline silicon substrate with a thin buffer layer ( $\sim 3\text{--}6$  nm) of silicon dioxide in-between. These samples were highly implanted with arsenic ions at a dose of  $5 \times 10^{16} \text{ cm}^{-2}$  and implantation energy of 100 KeV. Following implantation these samples were annealed for 1 h in nitrogen at temperatures ranging from 300 to 1100  $^{\circ}\text{C}$ .

The ellipsometer is an instrument that allows full characterization of the optical properties of thin films. Using the

ellipsometric parameters  $\tan \Psi$  and  $\cos \Delta$  [9], where  $\Psi$  and  $\Delta$  are the ellipsometric angles that describe the reflection of the polarized light, the thickness and the dielectric functions of the sample, can be determined using appropriate optical/structural models.

### 3. Results and discussion

The ellipsometric spectra were acquired in the spectral range of 240–840 nm with steps of 5 nm at an incident angle of  $75^{\circ}$ . The experimental results are represented in Fig. 1a–1f by full circles. From these graphs we see that there is a clear difference between non-annealed or low temperature annealed samples (spectra 1a–1b) and samples annealed at high temperatures

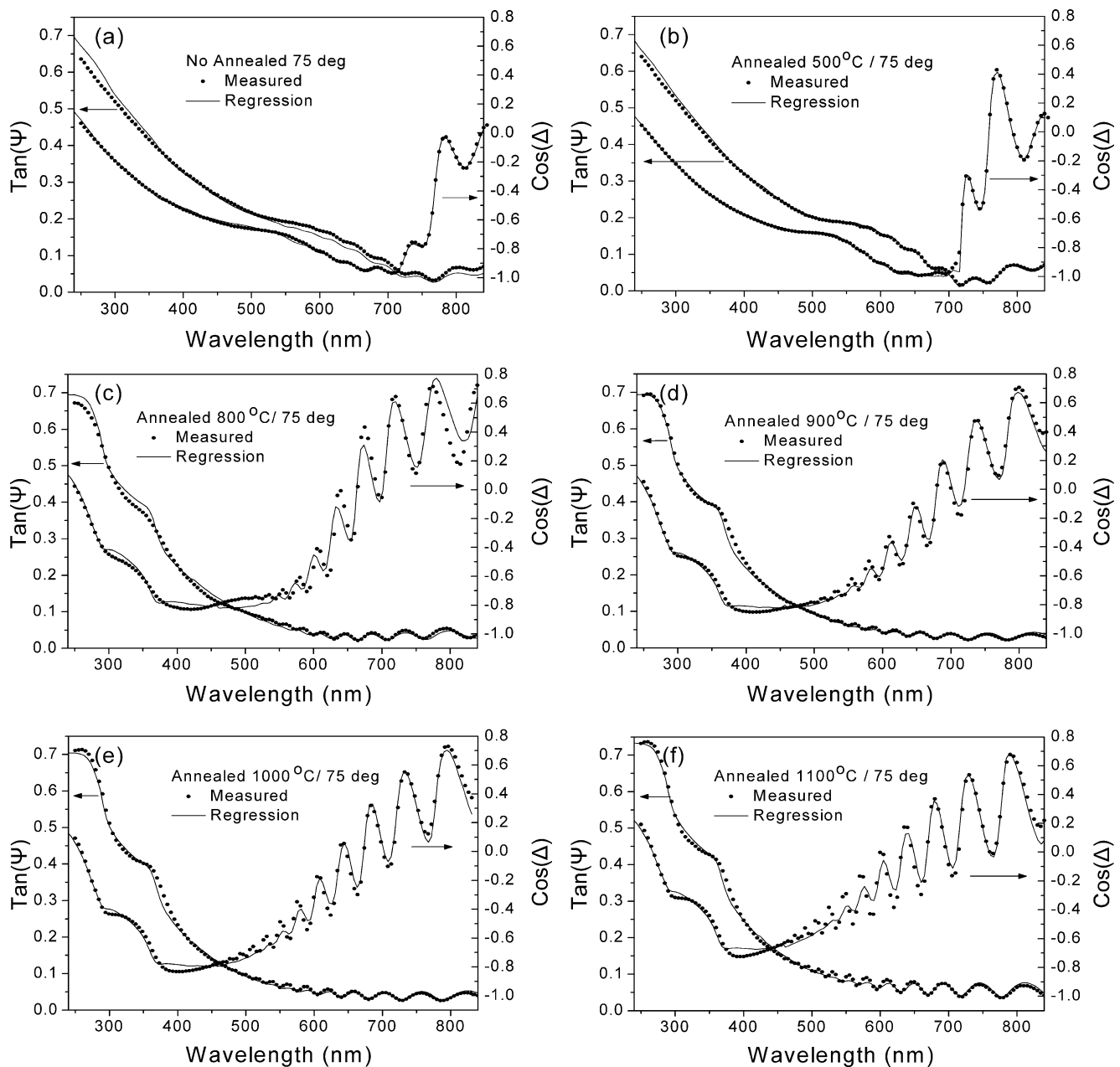


Fig. 1. Measurements (full circles) and regression results (solid line) for both ellipsometric parameters  $\tan \Psi$  and  $\cos \Delta$  as a function of wavelength are presented. The samples are annealed up to 1100  $^{\circ}\text{C}$  and the incident angle is  $75^{\circ}$ .

(spectra 1c–1f). The strong oscillatory behavior appearing in the  $\cos \Delta$  spectra and more pronounced in high temperature annealed samples is due to the interface between materials with different refractive indices.

Using Monte Carlo simulations for ion implantation [10] we have been able to reconstruct the amorphization profile of the non-annealed sample. The penetration depth of arsenic ions in silicon with implantation energy of 100 keV and a dose of  $5 \times 10^{16} \text{ cm}^{-2}$  has been found to be approximately  $0.17 \mu\text{m}$  (see Fig. 2). The high dose used in this work results in three distinct regions represented in Fig. 2 by R1, R2 and R3. The first region (R1) corresponds to a thin top layer ( $<2.5 \text{ nm}$ ) where the density of the induced damage is below the critical amorphization density ( $N_c = 5 \times 10^{22} \text{ atoms/cm}^3$ ). We note that the critical amorphization density in the TRIM calculations is the density of crystalline silicon. This in effect suggests that part of this sample remains in crystalline form. As a matter of fact we will demonstrate from the ellipsometry data that it is due to the small layer size that this region behaves like crystalline silicon. The second region (R2) corresponds to the layer ( $<0.1 \mu\text{m}$ ) where the sample sustained extensive damage from the ion implantation. In this region the density of the ion-induced vacancies is larger than the critical amorphization density ( $N_c$ ) and as a result the sample is considered to be completely amorphous. We should point out that the density of ion-induced vacancies refers to vacancy–interstitial pairs (Frenkel pairs) [11]. The amorphization in crystalline silicon is much more complex than simply vacancy formation. It entails formation of Frenkel pairs, point defects and amorphous nanoclusters [12] where collision cascades are located. Finally the third region (R3) corresponds to a layer approximately  $0.07 \mu\text{m}$  thick where the sample sustained partial damage. The density of the ion-induced vacancies is lower than the critical amorphization density, therefore the sample in this region is considered partially amorphous. The region below the R3 layer corresponds to the residual polycrystalline silicon, which is unaffected by the ion implantation.

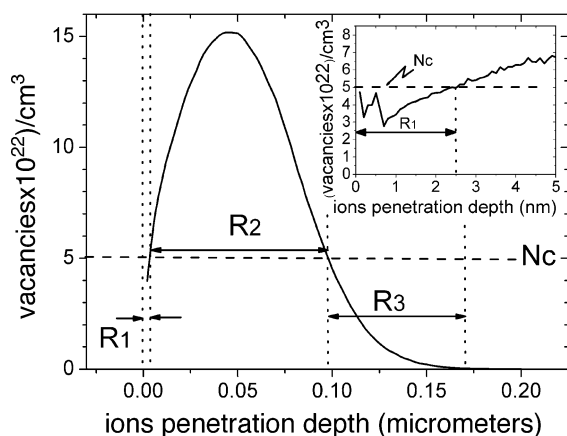


Fig. 2. Reconstruction of the amorphization profile using Monte Carlo simulation of the arsenic ion implantation in silicon with implantation energy of 100 keV and a dose of  $5 \times 10^{16} \text{ cm}^{-2}$ . The high dose used in this work results in three distinct regions represented by R1, R2 and R3. The horizontal line represented by  $N_c$  corresponds to the critical amorphization density.

Table 1

Thickness and concentrations of the regions from the regression fitting results for non-annealed and low annealed samples (up to  $500 \text{ }^\circ\text{C}$ )

| Regions    | Material         | Thickness (nm) | Thickness                    | Thickness                    | Thickness                    |
|------------|------------------|----------------|------------------------------|------------------------------|------------------------------|
|            |                  | Non-annealed   | (nm)<br>300 $^\circ\text{C}$ | (nm)<br>400 $^\circ\text{C}$ | (nm)<br>500 $^\circ\text{C}$ |
| 1          | SiO <sub>2</sub> | 4.1            | 3.9                          | 4                            | 3.2                          |
|            | c-Si/a-Si        | 2.5            | 2.5                          | 2.5                          | 2.5                          |
|            | Conc. a-Si       | 81.9%          | 82.0%                        | 86.9%                        | 92.7%                        |
| 2          | a-Si             | 84.8           | 84.8                         | 84.8                         | 84.8                         |
|            | pc-Si/a-Si       | 40.8           | 40.8                         | 40.8                         | 40.8                         |
| 3          | Conc. a-Si       | 30.5%          | 17.38%                       | 13.27%                       | 5.29%                        |
|            | pc-Si            | 945            | 986                          | 964                          | 943                          |
| Main layer | SiO <sub>2</sub> | 1.5            | 2.1                          | 2.5                          | 2.9                          |
|            | c-Si             | –              | –                            | –                            | –                            |

To further investigate and analyze the optical properties of the above films we used an optical structural model to fit the experimental data obtained from the ellipsometry. Monte Carlo simulations indicate that a basic structural model corresponding to the ion-induced damage region consists of three layers (R1, R2 and R3 as described above). Based on this information the optical structural model that we have adapted for our samples consists of a native oxide surface layer ( $\sim 4 \text{ nm}$  thick), regions 1, 2 and 3, as we have described above, a  $\sim 0.83 \mu\text{m}$  thick residual polycrystalline silicon, a buffer silicon oxide layer (3 nm) and the crystalline silicon which is the substrate of the samples. In this work we used the Bruggeman effective medium approximation (BEMA) [13] to represent the effective optical properties of the three layers made from a mixture of amorphous and polycrystalline silicon.

The utilized fitting process is the nonlinear Levenberg–Marquardt regression method and the standard deviation is defined by the formula

$$\sigma = \left\{ \frac{1}{(N - P - 1)} \sum_{j=1}^N \left[ \left( \cos \Delta_j^{\text{meas}} - \cos \Delta_j^{\text{regr}} \right)^2 + \left( \tan \psi_j^{\text{meas}} - \tan \psi_j^{\text{regr}} \right)^2 \right] \right\}^{1/2},$$

where  $N$  is the number of independently measured values corresponding to different wavelengths and  $P$  is the number of unknown model parameters. (Here “meas” and “regr” refer to

Table 2

Thickness and concentrations of the regions from the regression fitting results for high annealed samples ( $800\text{--}1100 \text{ }^\circ\text{C}$ )

| Regions    | Material         | Thickness                    | Thickness                    | Thickness                     | Thickness                     |
|------------|------------------|------------------------------|------------------------------|-------------------------------|-------------------------------|
|            |                  | (nm)<br>800 $^\circ\text{C}$ | (nm)<br>900 $^\circ\text{C}$ | (nm)<br>1000 $^\circ\text{C}$ | (nm)<br>1100 $^\circ\text{C}$ |
| 1          | SiO <sub>2</sub> | 3.4                          | 3.1                          | 3.8                           | 6.1                           |
|            | c-Si             | 2.5                          | 2.5                          | 2.5                           | 2.5                           |
| 2–3        | pc-Si/a-Si       | 17.7                         | 17.7                         | 17.7                          | 17.7                          |
|            | conc. a-Si       | 20.5%                        | 8.42%                        | 7.92%                         | 8.16%                         |
| Main layer | pc-Si            | 970                          | 1000                         | 1010                          | 990                           |
|            | SiO <sub>2</sub> | 2.1                          | 1.7                          | 2.5                           | 4                             |
| Substrate  | c-Si             | –                            | –                            | –                             | –                             |

measured and regression values, respectively). The regression results of ellipsometric parameters  $\tan \Psi$  and  $\cos \Delta$  at an incident angle of  $75^\circ$  are shown in Fig. 1 by a solid line. It is clear that the regression results for all samples under investigation in this work fit well to the experimental data at various annealed temperatures. Tables 1 and 2 show the various fitting parameters of the structural model from the regression results for the low and high annealing temperature samples, respectively.

We should point out that for the non-annealed and low annealed samples (Table 1) the thickness of the regions 1, 2

and 3 defined in our structural model was kept constant thus obtaining a comparison of the concentration mixtures between the various phases of silicon in these regions with increasing annealing temperature. When the thickness in the regression process was allowed to vary, we noticed a gradual decrease in the size of regions 1 and 3 due to recrystallization of the amorphous phase of silicon as expected. On the other hand, regression results reveal that region 2 maintained a constant thickness up to  $500^\circ\text{C}$ . This was to be expected since the ion-induced amorphous silicon sustained a major

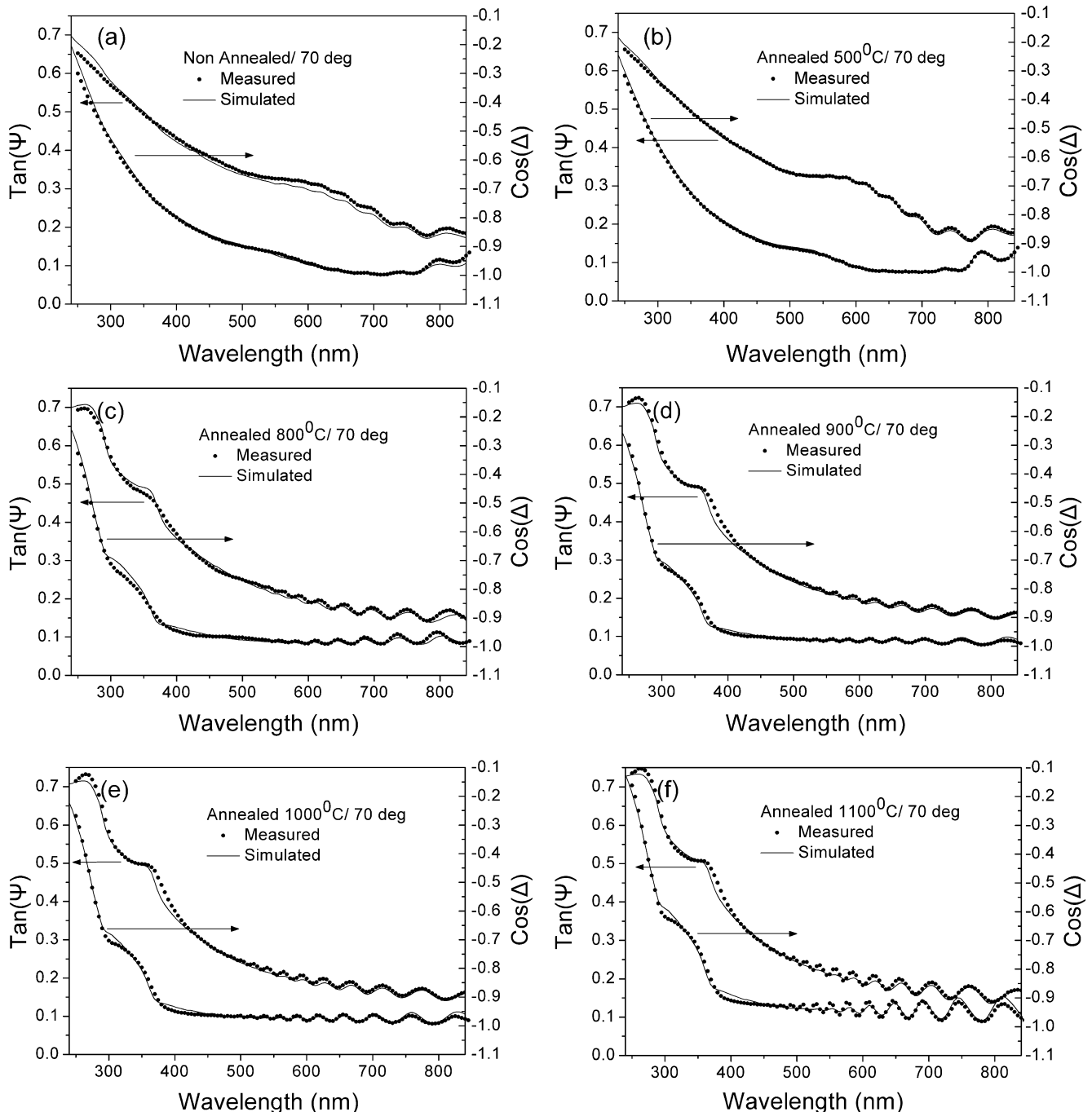


Fig. 3. Measured (full circles) and simulated data (solid line) for both ellipsometric parameters  $\tan \Psi$  and  $\cos \Delta$  as a function of wavelength. The samples are annealed up to  $1100^\circ\text{C}$  and the incident angle is  $70^\circ$ .

damage. For the higher annealing samples, the thickness in the regression was considered constant so as to allow a comparison of the amorphous silicon concentrations with increasing annealing temperature. When the thickness was allowed to vary, we noticed a very small change in the thickness as a function of temperature.

To further investigate and to confirm the validity of our optical models we have performed ellipsometric measurements at a different incident angle. In Fig. 3 we present the data (full circles) and the simulation results (solid lines) at the incident angle of  $70^\circ$ , using the optical models seen in Tables 1 and 2, which we extracted from the regression process at the incident angle of  $75^\circ$ . It appears that the simulated curves fit well with the experimental measurements. We should point out that simulation curves fit also well with other incident angles. This confirms the validity of our structural models for these samples following annealing at various temperatures.

It should be mentioned that the dielectric functions of the amorphous (a-Si), polycrystalline (pc-Si) and crystalline silicon (c-Si) used in this work were experimentally obtained from reference samples using spectroscopic ellipsometry and are plotted in Fig. 4. The results are in good agreement with that given in Refs. [14] and [15].

Next we analyze the regression results in more detail. Starting at region 3 (the inner ion-induced damaged layer) we notice this layer consists of a mixture of 30% a-Si and 70% pc-Si. This mixture ratio agrees with the estimated value obtained from the Monte Carlo simulations for the non-annealed sample. With increasing annealing temperature, the amorphous concentration diminishes reaching a value of  $\sim 5.3\%$  at  $500^\circ\text{C}$ . At  $800^\circ\text{C}$  and higher annealing temperatures region 3 recrystallize completely. On the other hand, region 2 which sustained the maximum damage from ion implantation remains amorphous even up to annealing temperatures of  $500^\circ\text{C}$ . At the annealing temperatures of  $800^\circ\text{C}$  and higher the thickness of this region becomes smaller due to the recrystallization of the amorphous layer. Finally, region 1 which is a very thin layer appears to behave like crystalline silicon. This behavior is evident at the higher annealed samples where most of the ion damage is removed and we notice the characteristic crystalline behavior in the shapes of the ellipsometry parameters for the short wavelength spectra range (see Fig. 1).

Using the proportion of silicon phases and the composition of each layer as a function of thickness we were able to extract the dielectric functions of the samples under investigation in this work (Fig. 4). The dielectric functions of non-annealed and low-temperatures-annealed samples (up to  $500^\circ\text{C}$ ) in a depth of  $0.1\ \mu\text{m}$  appear to approach the line shape of amorphous silicon. This was expected since the ion implantation damaged the polycrystalline silicon samples resulting in an amorphous silicon layer ( $\sim 0.1\ \mu\text{m}$  near the surface). As the annealing temperature increases the samples appear to be converted into polycrystalline silicon as the curves of Fig. 4 show. This is attributed to the recrystallization of the samples at these annealing temperatures ( $500$

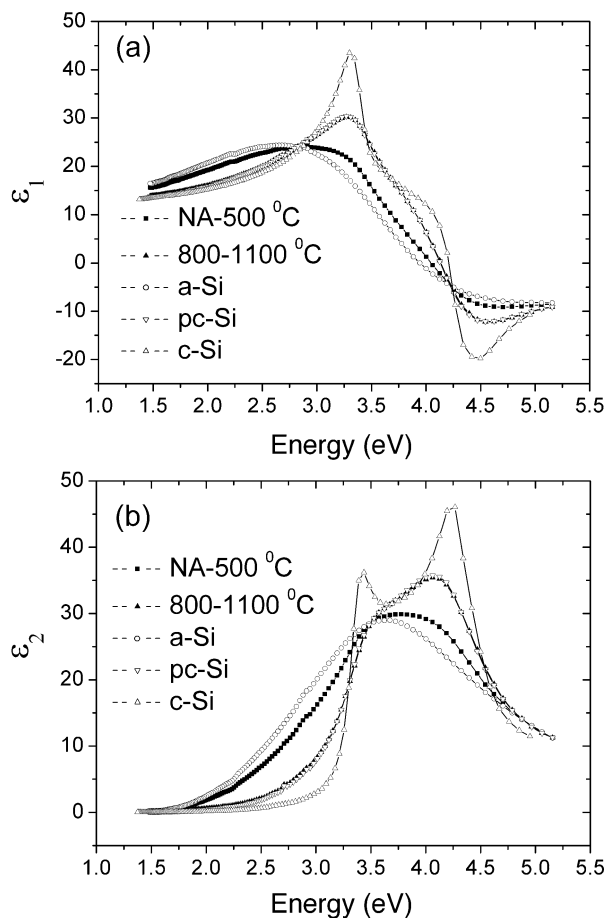


Fig. 4. The dielectric functions of low and high annealed samples of the ion-induced damaged region. For comparison purposes, we present the dielectric functions of the reference materials (c-Si, a-Si, pc-Si).

$800^\circ\text{C}$ ). Finally, we should point out that the dielectric functions obtained at the various incident angles were in excellent agreement. This further supports the validity of our structural/optical model.

#### 4. Conclusion

We have demonstrated the sensitivity of the ellipsometric parameters  $\tan \Psi$  and  $\cos \Delta$  in the  $240\text{--}840\ \text{nm}$  spectral range on ion-implanted polycrystalline silicon films before and after annealing at various temperatures. The ion-induced damage region was reconstructed using simple Monte Carlo simulations, estimating the penetration of arsenic ion in silicon and the amorphization regions of the samples. Based on this information we have constructed an optical/structural model for all the annealed samples, where the Bruggeman effective medium approximation was used in obtaining the various mixture profiles of silicon phases. Regression results obtained from the fitting experimental parameters based on the optical/structural model for the samples provided valuable information given by the depth profiling ability of spectroscopic ellipsometry and the temperature-evolution of the ellipsometric results.



## References

- [1] P. Petrik, T. Lohner, M. Fried, N.Q. Khánh, O. Polgár, J. Gyulai, *Nucl. Instrum. Methods Phys. Res., B Beam Interact. Mater. Atoms* 147 (1999) 84.
- [2] P. Petrik, O. Polgár, T. Lohner, M. Fried, N.Q. Khánh, J. Gyulai, *Vacuum* 50 (1998) 293.
- [3] X.Z. Bo, N. Yao, S.R. Shieh, T.S. Duffy, J.C. Sturm, *J. Appl. Phys.* 91 (2002) 2910.
- [4] D.E. Aspnes, A.A. Studna, E. Kinsborn, *Phys. Rev., B* 29 (1984) 768.
- [5] K. Vdam, P.J. McMarr, J. Narayan, *Appl. Phys. Lett.* 47 (1985) 339.
- [6] M. Fried, T. Lohner, J.M.M. de Nijs, A. van Silfhout, L.J. Hanekamp, Z. Laczik, N.Q. Khánh, J. Gyulai, *J. Appl. Phys.* 66 (1989) 5052.
- [7] J. Vanhellemont, H.E. Maes, A. De. Veirman, *J. Appl. Phys.* 65 (1989) 4454.
- [8] E. Lioudakis, A. Othonos, *Opt. Eng.* 44 (2) (2005) 023802.
- [9] R. Azzam, N. Bashara, North-Holland Publishing (1977) 66.
- [10] J.F. Ziegler, J.P. Biersack and U. Littmark, *The Stopping Range of Ions in Solids*, Pergamon, Tarrytown, New York, (1985) and J.F. Ziegler and J.P. Biersack, TRIM software, SRIM-version 2003.26 (<http://www.srim.org/>).
- [11] W.J. Weber, *Nucl. Instrum. Methods Phys. Res., B Beam Interact. Mater. Atoms* 166–167 (2000) 98.
- [12] W.J. Weber, F. Gao, R. Devanathan, W. Jiang, C.M. Wang, *Nucl. Instrum. Methods Phys. Res., B Beam Interact. Mater. Atoms* 216 (2004) 25.
- [13] D.E. Aspnes, *Thin Solid Films* 81 (1981) 249.
- [14] G.E. Jellison Jr., M.F. Chisholm, S.M. Gorbalkin, *Appl. Phys. Lett.* 62 (1993) 3348.
- [15] G.E. Jellison Jr., *Opt. Mater.* 1 (1992) 41.